cDC1 and interferons promote spontaneous CD4$^+$ and CD8$^+$ T cell protective responses to breast cancer

Raphaël Mattiuz[1], Carine Brousse[1], Marc Ambrosini[1], Jean-Charles Cancel[1], Gilles Bessou[1], Julie Mussard[2], Amélien Sanlaville[2], Christophe Caux[2], Nathalie Bendriss-Vermare[2], Jenny Valladeau-Guilemond[2], Marc Dalod[1*], Karine Crozat[1*]

Author affiliations:

[1]Centre d'Immunologie de Marseille-Luminy, Turing Center for Living Systems, CNRS, INSERM, Aix Marseille Univ, Marseille, France

[2]Univ Lyon, Université Claude Bernard Lyon 1, INSERM 1052, CNRS 5286, Centre Léon Bérard, Cancer Research Center of Lyon, Lyon, France.

*Equal contribution and correspondence: Marc Dalod dalod@ciml.univ-mrs.fr, Karine Crozat crozat@ciml.univ-mrs.fr

Running title (58 characters): cDC1 and IFNs promote spontaneous control of breast cancer

Keywords: cDC1, Cancer immunosurveillance, Interferons, IFN-γ, CD4$^+$ T cells, CD8$^+$ T cells, breast cancer

Conflicts of Interest: The authors declare no potential conflicts of interest.

Manuscript length: 7 main figures; 6,518 characters for (introduction; materials and methods, results, discussion and figure legends); 52 references.

Synopsis (38 words)

Type 1 conventional dendritic cells cross-present tumor antigens to $CD8^+$ T cells. Understanding the regulation of their antitumor functions is important. Cell-intrinsic STAT1/IFN-γ signaling licenses them for efficient $CD4^+$ and $CD8^+$ T cell activation during breast cancer immunosurveillance.

Abstract (219 words)

Here we show that efficient breast cancer immunosurveillance relies on cDC1, conventional $CD4^+$ T cells, $CD8^+$ cytotoxic T lymphocytes (CTL) and later NK/NK T cells. For this process, cDC1 were required constitutively, but especially during the T cell priming phase. In the tumor microenvironment, cDC1 interacted physically and jointly with both $CD4^+$ T cells and tumor-specific $CD8^+$ T cells. We found that interferon (IFN) responses were necessary for the rejection of breast cancer, including cDC1-intrinsic signaling by IFN-γ and STAT1. Surprisingly, cell-intrinsic IFN-I signaling in cDC1 was not required. cDC1 and IFNs shaped the tumor immune landscape, notably by promoting $CD4^+$ and $CD8^+$ T cell infiltration, terminal differentiation and effector functions. XCR1, CXCL9, IL-12 and IL-15 were individually dispensable for breast cancer immunosurveillance. Consistent with our experimental results in mice, high expression in the tumor microenvironment of genes specific to cDC1, CTL, helper T cells or interferon responses are associated with a better prognosis in human breast cancer patients. Our results show that immune control of breast cancer depends on cDC1 and IFNs as previously reported for immunogenic melanoma or fibrosarcoma tumor models, but that the underlying mechanism differ. Revisiting cDC1 functions in the context of spontaneous immunity to cancer should help defining new ways to mobilize cDC1 functions to improve already existing immunotherapies for the benefits of patients.

Introduction

Conventional dendritic cells (cDC) are specialized in antigen (Ag) capture, processing and presentation for T cell priming (1). cDC are present in lymphoid organs and peripheral tissues. Lymphoid resident-cDC (Res-cDC) of the spleen and lymph nodes (LNs) participate in the capture of Ag from blood and lymph respectively. cDC in non-lymphoid tissues capture Ag at the periphery and migrate to the LNs via the afferent lymphatic vessels. cDC encompass two distinct cell types. Type 1 cDC (cDC1) excel in cytotoxic $CD8^+$ T cell (CTL) activation, particularly via Ag cross presentation (2-4). Type 2 cDC (cDC2) are particularly effective for helper $CD4^+$ T cell activation (1).

Previous studies suggested that cDC1 play a non-redundant role in anti-tumor immunity, both for spontaneous control of syngeneic tumor grafts used as a surrogate model for cancer immunosurveillance, and for rejection of established tumors upon immunotherapy (5,6). Yet, most of these studies used mutant mice whose deficiencies were not affecting exclusively cDC1. *Irf8* deficiency in CD11c-expressing cells also affected the differentiation and functions of plasmacytoid dendritic cells (7) and inflammatory cDC2 (8). Batf3 knock-out does not only abrogate cDC1 differentiation (9) but was also recently shown to enhance $CD4^+$ regulatory T cell (Treg) induction (10) and to hamper CTL survival and memory (11,12) in a cell-intrinsic manner. Hence, mouse models targeting cDC1 with a higher specificity are mandatory to investigate whether and how they contribute to antitumor immunity (11). This is the case of mice knocked-in for the Cre recombinase in the *Xcr1* locus (13).

A number of key features of cDC1 are proposed to contribute to their critical role in antitumor immunity, beyond their efficiency at cross-presenting cell-associated antigens (5,6). cDC1 may have the unique ability to simultaneously deliver to CTLs a series of complementary output signals ensuring their optimal response. CXCL9 attracts CXCR3-expressing memory or effector CTLs to the tumors. IL-12 production and IL-15 trans-presentation promote CTL IFN-

γ expression and proliferation. cDC1 could also promote delivery to CTLs of help from other immune cells including $CD4^+$ T cells (5,14). However, which of these output signals are critical for cDC1 antitumor immunity remains to be rigorously investigated (5,15).

The antitumor functions of cDC1 has been proposed to depend on their integration of specific input signals, instructing them to deliver the right output signals to CTLs. cDC1 recruitment into the tumor bed can be promoted by engagement of their chemokine receptor Xcr1 (16), whose ligand Xcl1 is produced by activated NK cells and CTLs (17). Triggering of the receptor for type I interferons (IFNAR) on cDC1 is necessary for rejection of immunogenic melanoma and fibrosarcoma by promoting Ag cross-presentation (18,19). It also boosts their expression of co-stimulation molecules, induces their trans-presentation of IL-15, and can promote their production of IL-12 (5,20). However, whether these input signals are always required by cDC1s for their antitumor functions is unknown. Moreover, to which extent and how different types of interferons promote the immunogenic maturation of cDC1, not only IFN-I but also IFN-III or IFN-γ, remains to be formally investigated.

Here, we studied whether cDC1 promote spontaneous immunity to breast cancer, and when, where and how this is achieved. To this aim, we used a mouse model of spontaneous immune control of breast cancer in C57BL/6 female mice, consisting of an orthotopic graft of a subclone of the NOP23 syngeneic breast adenocarcinoma cell line expressing epitopes from the ovalbumin (OVA) model antigen (21). This experimental system enabled us to study the cellular and molecular mechanisms underpinning spontaneous immune control of breast cancer, by harnessing the *Karma-tmt-hDTR* (22), *Xcr1-DTA*, $Xcr1^{Cre}$ and $Karma^{Cre}$ (13) mutant mouse models that we have generated and validated to specifically target cDC1, in combination with other mutant C57BL/6 mice.

Materials and Methods

Ethics statement regarding care and use of animals for experimentation

Mice were bred and maintained the CIPHE pathogen-free animal facility. The study was carried out in accordance with institutional guidelines and with protocols approved by the Comité National de Réflexion Ethique sur l'Expérimentation Animale #14 and the Ministère de l'Enseignement Supérieur, de la Recherche et de l'Innovation (ROXinAIR APAFiS #1221 and #16555).

Mice and in vivo treatments

All experiments were performed with female littermate mice at 7–15 weeks of age. The mouse strains used are all on the C57BL/6J background and listed in Table S1. For a sustained and efficient cDC1 conditional depletion for at least 10 consecutive days, *Karma-tmt-hDTR* and *Xcr1*$^{Cre/wt}$;*Rosa26*$^{hDTR/wt}$ mice received a first dose of 32 ng/g of body weight of DT (Merck), followed by one injection of 16 ng/g every 60h. For *in vivo* antibody-mediated cell depletion, C57BL/6 mice were injected i.p. with the antibody and doses indicated in Table S2, starting 1d before tumor engraftment and then as indicated in the figures. To block lymphoid cell egress from peripheral lymphoid organs, mice received 20 µg of FTY720 (Cayman Chemical) starting 1d before tumor engraftment, then every 2d.

Tumor experiments

We used a breast adenocarcinoma tumor cell line that is spontaneously rejected when orthotopically implanted in C57BL/6 females. It was derived from the NOP23 cell line, which was established from a spontaneous mammary tumor of a transgenic mouse expressing a dominant negative version of p53 and the rat NEU (HER2) oncogene fused at its COOH terminus to class I and II OVA peptide sequences (21). NOP23 cells were grown in DMEM,

10% FCS, supplemented with 10mg/ml of Insulin transferrin Sodium Selenite media supplement (Sigma-Aldrich). 5.10^6 NOP23 cells were injected in the mammary inguinal fat pad, under isoflurane anesthesia. Tumor volume was calculated as $\frac{\pi}{6} \times L \times W^2$, where L is the greatest length and W is the width of the tumor, measured with a caliper. Graphs of tumor volume are represented as mean+/-SEM.

Shield bone marrow chimera mice

To generate *Ifngr1*$^{-/-}$→*Xcr1*-DTA and *Stat1*$^{-/-}$→*Xcr1*-DTA shield bone marrow chimera (SBMC) mice, the hind legs of *Xcr1*-DTA recipient mice were irradiated with one dose of 8 Gy, to preserve most of their hematopoietic system that remained WT. The cDC1 empty niche of these recipient mice was then reconstituted upon injection of 30.10^6 bone marrow cells from *Ifngr1*$^{-/-}$ or *Stat1*$^{-/-}$ donor mice. *Xcr1*-DTA→*Xcr1*-DTA and WT→*Xcr1*-DTA SBMC mice were used as controls. NOP23 cells were engrafted 8 to 14 weeks later.

Preparation of cell suspension from tumors and TdLNs for flow cytometry

Tumors and tumor-draining inguinal LNs (TdLNs) were cut into small pieces with a scalpel and incubated in a Collagenase D (1 mg/ml)/ of DNase I (70 µg/ml) enzymatic cocktail (Roche) in RPMI, for 30min at 37°C. Ice-cold PBS/EDTA (2 mM) was added for 5 min. Digested tissues were crushed through a 70 µm nylon sieve. For flow cytometry, cells were pre-incubated with 2.4G2 mAb to block Fc-receptors, then stained with the mAb listed in Table S2 for 25 min at 4°C. Class-I OVA Tetramer (iTAg Tetramer/PE - H-2 Kb OVA [SIINFEKL], MBL International) was incubated at 1/100 at 4°C for 1 hour, and Class-II OVA Tetramer (T-Select I-Ab OVA323-339 [ISQAVHAAHAEINEAGR] Tetramer-APC, MBL International) at 1/12.5 at room temperature for 1 hour, before proceeding to staining with mAbs. For CCR7 staining, cells were incubated for 30 min at 37°C. For intracellular staining, cells were re-stimulated *ex*

149 *vivo* for 4h at 37°C with 0.5 µg/ml of SIINFEKL peptide and 10 µg/ml of Brefeldin A (Sigma-
150 Aldrich) in complete RPMI. Cytokines, Ki67 and FoxP3 were stained after
151 fixation/permeabilization with FoxP3/Transcription Factor Staining Buffer Set (eBioscience).
152 Data were acquired on a LSRFortessa X-20 flow cytometer (BD Biosciences), and analyzed
153 using FlowJo (Tree Star, Inc.). Flow cytometry heatmaps were performed using the Morpheus
154 website from the Broad Institute (https://software.broadinstitute.org/morpheus/).
155
156 **Immunohistofluorescence**
157 1,000 naive GFP-expressing OT-I cells were purified from a $Tg^{TcraTcrb1100Mjb};Rag2^{-/-};Ubc\text{-}GFP^{+/+}$ spleen with the Dynabeads Untouched Mouse CD8 Cells Kit (ThermoFisher Scientific)
158
159 and transferred i.v. in $Xcr1^{Cre/wt};Rosa26^{tdRFP/wt}$ mice 1d before tumor engraftment. 7d after,
160 tumors were harvested and 12-µm frozen sections were stained with the antibodies listed in
161 Table S2, as described previously (23).
162
163 **Quantitative PCR analysis**
164 Total RNA from tumors and TdLNs were prepared with the RNeasy Plus mini kit (QIAGEN).
165 RNA was reverse transcribed into cDNA using the QuantiTect reverse transcription kit
166 (QIAGEN). qPCR was performed with the SybrGreen kit (Takara) and specific primers (Table
167 S3), and run on a 7500 Real Time PCR System apparatus (Applied Biosystems). Relative gene
168 expression was calculated using the ΔΔCt method with *Hprt* as housekeeping control gene.
169
170 **Transcriptomic data from breast cancer patients**
171 *XCR1* Kaplan Meier plot was obtained from the Kaplan Meier-plotter database
172 (https://kmplot.com/analysis/), and *CCR7* and *CCL19* Kaplan Meier plots from The Cancer
173 Genome Atlas (TCGA) database. Transcripts enriched in tumors of breast cancer patients with

a better overall survival (367 genes) or with a poor prognosis (210 genes) from TCGA were extracted through the human protein atlas (https://www.proteinatlas.org/humanproteome/pathology). A gene is considered prognostic if correlation analysis of gene expression and clinical outcome resulted in Kaplan-Meier plots with high significance ($p<0.001$). The gene ontology analyses on the good and bad prognosis gene lists were performed with DAVID 6.8 (https://david.ncifcrf.gov/).

Statistical analyses

Statistical analyses were performed using unpaired Student's *t*-tests or nonparametric Mann-Whitney tests (MW) when specified. N.S., non-significant ($P>0.05$); *, $P\leq0.05$; **, $P\leq0.01$; ***, $P\leq0.001$, ****, $P\leq0.0001$.

Results

CTL, CD4$^+$ T_{conv} and NK1.1$^+$ cells are instrumental to rejection of NOP23 mammary tumors.

We first investigated whether T or NK cells were providing the effector arm of the spontaneous rejection of the NOP23 breast adenocarcinoma cells in C57BL/6J females. Tumor rejection was abolished by continuous depletion of CTLs or of NK1.1$^+$ cells (*i.e.* NK cells and a fraction of NKT cells) (**Fig. 1A**). However, the anti-NK1.1 mAb-mediated depletion showed a delayed and milder effect than CTL depletion. Continuous depletion of all CD4$^+$ T cells also abrogated tumor control (**Fig. 1B**), whereas this was not the case of the selective depletion of intra-tumor Treg as achieved with administration of the anti-CTLA-4 clone 9D9 (24). Thus, CTLs, CD4$^+$ conventional T cells (T_{conv}) and NK/NK T cells are required for NOP23 tumor rejection.

cDC1 are critical for breast cancer control, especially during the T cell priming phase.

We next examined, whether and when cDC1 depletion compromised the immune control of NOP23 growth, by taking advantage of our mutant mouse models specifically targeting cDC1. The *Xcr1*$^{Cre/wt}$;*Rosa26*$^{DTA/wt}$ (*Xcr1-DTA*) model (Mattiuz et al., 2018) harbored a constitutive and complete lack of all cDC1 in the spleen and IngLNs (**Fig. S1A-B**). The *Xcr1*$^{Cre/wt}$;*Rosa26*$^{hDTR/wt}$ (*Xcr1-hDTR*) mouse model allowed conditional depletion of cDC1 in spleen, and of Mig-cDC1 and Res-cDC1 in the inguinal lymph nodes (IngLNs), for at least 2 days following the administration of a single dose of diphtheria toxin (DT) (**Fig. S1A-B**), similarly to the *Karma-tmt-hDTR* (*Karma*) mice (Alexandre et al., 2016). None of the other immune cell types examined in the spleen and IngLNs were affected in these mice (**Fig. S1C**). *Xcr1-DTA* mice harbored a progressive and unabated growth of NOP23 as compared to control WT animals (**Fig. 2A**), demonstrating that cDC1 are necessary to efficiently reject this breast

adenocarcinoma. To determine when cDC1 were required to promote this rejection, we conditionally depleted these cells in *Karma* mice during different time windows relative to tumor engraftment (**Fig. 2A**). The earlier the depletions were initiated, the stronger the tumors grew. However, the tumors never grew as strongly as in the *Xcr1-DTA* mice that are constitutively devoid of cDC1 (**Fig. 2A-B**). TdLN mig-cDC1 showed a high expression of the co-stimulatory molecules CD40 and CD86 at day 4 post-engraftment, as compared to Res-cDC1 or to Mig-cDC1 on any other days (**Fig. 2C**). In summary, cDC1 were required continuously until tumor rejection, but their presence was especially critical during the first 4 days after tumor engraftment, most likely during the phase of T cell priming.

CCR7- and S1PR1-dependent immune cell trafficking is instrumental to NOP23 rejection.

At day 7 post-engraftment, CCR7 was upregulated on cDC1 that had migrated from the periphery into the TdLN (**Fig. S2A**). We thus investigated whether CCR7-dependent immune cell trafficking was critical for NOP23 rejection. In *Ccr7*$^{-/-}$ mice, the NOP23 tumor grew uncontrolled (**Fig. S2B**). Blocking lymphocyte egress from secondary lymphoid organs with the sphingosine-1-phosphate receptor (S1PR1) inhibitor FTY720 (25) also abrogated spontaneous tumor control (**Fig. S2C**). It reduced intra-tumor infiltration of lymphocytes as compared to control animals or to mice depleted of CTLs or NK1.1^{+} cells (**Fig. S2D**). Taken together, these results suggested that two-way traffic of immune cells between the periphery and TdLNs was critical for the establishment of an effective endogenous anti-tumor immune response within the TME.

cDC1 interact with CD4^{+} T cells and tumor-specific CTLs in the TME.

Because cDC1, CTL and CD4^{+} T_{conv} were all critical to trigger NOP23 rejection, we wondered whether cDC1 interacted with T cells in the TME. To follow the behavior of Ag-specific CTLs

in our experimental models, 1d before tumor engraftment we adoptively transferred low numbers (1,000) of naïve GFP-expressing OT-I cells into *Xcr1*$^{Cre/wt}$;*Rosa26*$^{tdRFP/wt}$ mice that allow in situ visualization of cDC1 by microscopy due to their specific expression of the RFP fluorescent reporter protein (**Fig. S3**). At d7 in the tumor bed, RFP$^+$ cDC1 were engaged in cell-cell contacts with both CD4$^+$ T cells and anti-tumor CTLs, in close proximity to the HER2$^+$ NOP23 cells (**Fig. 3**). This suggested that, in the tumor stroma, cDC1 simultaneously cross-presented tumor Ags to CTLs and relayed them the CD4$^+$ T_{conv} help.

CXCL9 and IL-12 production by cDC1, as well as their trans-presentation of IL-15, are individually dispensable for the immune control of NOP23 tumors.

To dissect how cDC1 promoted spontaneous immune control of NOP23, we first tested the candidate molecules CXCL9, IL-12 and IL-15, which had been proposed to be key output signals delivered by cDC1 to T or NK/NK T cells for their recruitment in the tumor or the activation of their effector functions (5). The NOP23 tumors were controlled in *Cxcl9*$^{-/-}$, *Il12b*$^{-/-}$ and *Il15ra*$^{-/-}$ mice as efficiently as in control mice (**Fig. 4A**). Consistent with these results, conditional inactivation of *Cxcl9* or *Il15ra* in cDC1 had no impact on tumor growth (**Fig. S4**). Thus, CXCL9 or IL-12 production and IL-15 transpresentation by cDC1 were not required individually for breast cancer rejection in our experimental settings.

IFN-I and IFN-γ responses, but not XCR1, are necessary for NOP23 tumor control.

We next sought to identify the input signals received by cDC1 and promoting their anti-tumor functions. *Xcr1*$^{-/-}$ mice efficiently controlled the NOP23 tumor cells (**Fig. 4A**). Hence, XCR1-dependent recruitment of cDC1 to the tumor bed (16) or micro-anatomical attraction to XCL1-producing effector lymphocytes within the tissue (23) was not necessary for breast tumor elimination in our experimental settings. To assess functionally the importance of IFN-I and

IFN-γ signaling in NOP23 control, we compared tumor growth between WT animals and *Ifnar1*$^{-/-}$, *Ifngr1*$^{-/-}$ or *Stat1*$^{-/-}$ mice, respectively lacking the ability to respond to IFN-I, to IFN-γ or to all types of IFNs including type III IFNs (IFN-III). All three mutant mice failed to control tumor growth, with a more pronounced effect in *Stat1*$^{-/-}$ mice (**Fig. 4B**). Thus, both IFN-I and IFN-γ were promoting antitumor immunity in the NOP23 breast cancer model. The analysis of the kinetics of induction of the *Ifna4, Ifna2* and *Ifnb1* genes and of interferon-stimulated genes (ISGs) showed that IFN-I responses were induced in the tumor within the first day after engraftment before rapidly decreasing, while they remained generally low in the TdLNs (**Fig. 4C** and **Fig. S5**). Conversely, *Ifng* expression increased gradually over time and was higher in the TdLNs than in the tumors (**Fig. 4C**). These results suggested that distinct IFNs and ISGs could have complementary roles at different times and locations to initiate and maintain protective anti-tumor immune responses.

The anti-tumor protective effects of IFN-γ and STAT1 occur at least in part in cDC1, whereas cDC1-intrinsic signaling by IFN-I is dispensable for NOP23 control.

We next investigated whether the protective antitumor roles of IFNs were at least in part due to cell-intrinsic effects on cDC1s. NOP23 cells were efficiently rejected in *Xcr1*^{Cre}*;Ifnar1*$^{fl/KO}$ and *Karma*$^{Cre/wt}$*;Ifnar1*$^{fl/fl}$ mice that are deficient for IFN-I responsiveness selectively in cDC1 (**Fig. 4D** and **S6A**). Moreover, cDC1 maturation and tumor-specific CTL activation in tumors of *Xcr1*^{Cre}*;Ifnar1*$^{fl/KO}$ mice were similar to those in control tumors (**Fig. S6B-C**). Thus, in our experimental settings, cDC1-intrinsic signaling by IFN-I was dispensable for NOP23 control.

To determine whether IFN-γ or overall IFN responses in cDC1 were critical for their promotion of NOP23 rejection, we generated shield bone marrow chimera (SBMC) mice deficient selectively in cDC1 for key components of the corresponding signaling pathways, namely *Ifngr1*$^{-/-}$→*Xcr1-DTA* and *Stat1*$^{-/-}$→*Xcr1-DTA* animals. Tumors grew progressively in *Ifngr1*$^{-/-}$

287 →*Xcr1-DTA* SBMC mice, but to a lower extent than in *Stat1*$^{-/-}$→*Xcr1-DTA* SBMC mice that
288 harbored a progressive and unabated tumor growth, like *Xcr1-DTA* animals and *Xcr1-*
289 *DTA*→*Xcr1-DTA* SBMC mice (**Fig. 4E**). Thus, the beneficial antitumor effects of IFN-γ and
290 STAT1 signaling occurred at least in part in cDC1.
291 Compared to controls, Mig-cDC1 from *Ifnar1*$^{-/-}$ and *Ifngr1*$^{-/-}$ TdLNs expressed less CCR7, and
292 their Res-cDC1 were less mature with a decrease in CD40, CD80 and CD86 expression (**Fig.**
293 **4F**), contrasting with a higher expression of CD40 on Res-cDC2 at d4-7, and of CD80 on Mig-
294 cDC2 at d7 (**Fig. 4F**). cDC1 expressed less CD40 in the tumors from *Ifnar1*$^{-/-}$ and *Ifngr1*$^{-/-}$ mice
295 at d15 (**Fig. 4G**). This suggested that loss of IFN responses led to a defective cDC1 maturation
296 in the tumor and TdLNs, with a compensatory increase in cDC2 maturation that was not
297 sufficient to maintain protective antitumor immunity.
298
299 **cDC1 and IFNs promote the infiltration of the tumor and its draining lymph node by**
300 **protective over putatively deleterious immune cell types**
301 To better understand the respective roles of cDC1 and IFNs in the anti-tumor response, we
302 quantified different immune populations in control, *Ifnar1*$^{-/-}$, *Ifngr1*$^{-/-}$ and *Xcr1-DTA* tumor at
303 d4, d7 and d15 (**Fig. 5** and **S7A**). The overall immune cell infiltration in the tumors increased
304 between d4 and d7, the highest in WT mice as compared to mutant animals, and later decreased
305 in all mice (**Fig. 5A**). At d4, the major difference observed between mutant mice and WT
306 controls was a decrease in cDC1 (**Fig. 5B**). At this stage, the tumor was mainly infiltrated in all
307 mouse strains by neutrophils, macrophages and γδ T lymphocytes identified as CD8^{-} CD4^{-}
308 CD3ε^{+} cells (**Fig. S7A**). At day 7, the proportion of cDC1 and NK cells within immune cells
309 remained lower in mutant animals as compared to WT mice (**Fig. 5B-C** and **S7A**). In contrast,
310 the immune infiltrate from the tumors of mutant animals harbored increased proportion of Lin^{-}
311 Siglec-H^{-} CD64^{-} CD11c^{+} MHC-II^{-} cells (**Fig. 5D** and **S7A**), corresponding most likely to DC

312 precursors (26) or immature DC. As compared to WT controls, the mutant mice showed a slight
313 decrease in $CD8^+$ T cell proportion at d7 (**Fig. 5D-E** and **S7**), and a marked decrease in the
314 proportions of $CD4^+$ T cells mostly at d7 (**Fig. 5D, F** and **S7**). The delayed tumor growth
315 observed upon $NK1.1^+$ cell depletion as compared to CTL depletion (**Fig. 1A**) was consistent
316 with the late infiltration of the tumor by NK cells (**Fig. 5C**) and NK T cells (**Fig. 5G**) as
317 compared to T cells (**Fig. 5E-F).** The fraction of activated ($CD44^+$) CTLs in the immune
318 infiltrates remained lower in all mutant animals (**Fig. 5D** and **S7**). This was also the case for the
319 fraction of $CD4^+$ T cells in *Xcr1-DTA* mice (**Fig. 5D, F** and **S7**), and for the fraction of NK cells
320 in *Ifngr1*$^{-/-}$ animals (**Fig. 5C, D** and **S7**). Conversely, at d15, the proportion of neutrophils in
321 the immune infiltrates was much higher in mutant mice than in WT controls (**Fig. 5D**), even
322 though the absolute numbers of neutrophils in tumors decreased sharply over time (**Fig. S7A**).
323 In the TdLNs, the proportion of activated ($CD44^+$) CTL was lower at all times in *Xcr1-DTA*
324 and *Ifnar1*$^{-/-}$ mice (**Fig. S7B**). Neutrophils were increased over time in all mutant mice, and
325 monocytes or macrophages in *Xcr1*-DTA and *Ifngr1*$^{-/-}$ mice, as compared to WT animals (**Fig.**
326 **S7B**). Starting at d4, Mig-cDC1 accumulated less in *Ifnar1*$^{-/-}$ and *Ifngr1*$^{-/-}$ mice than in WT
327 animals (**Fig. S7B**). Conversely, the proportion of Mig-cDC2 increased over time (**Fig. S7B**).
328 This suggested that the early migration of cDC1 from the tumor to the TdLNs is IFN-dependent
329 and that its absence leads to a compensatory phenomenon of increased cDC2 migration from
330 the tumor to the TdLN.
331 Altogether, these results showed that IFNs and cDC1 contributed to sculpt the immune
332 composition of the tumor and TdLN by promoting a higher ratio of protective immune cells,
333 not only NK and CTL but also $CD4^+$ T_{conv}, over potentially deleterious myeloid cells including
334 macrophages and neutrophils. IFN effects on the tumor immune infiltration may have occurred
335 in part indirectly through promoting early cDC1 recruitment.
336

cDC1 and IFNs are necessary for CD4$^+$ T_{conv} and CTL terminal activation and effector functions in the TME

We then focused on tumor-specific (Tetramer$^+$) CD4$^+$ T cells and CTL responses. Their proportions within tumor-infiltrating immune cells did not differ between experimental groups (**Fig. 6A**). As compared to total T cells, tumor-infiltrating Tetramer$^+$ T cells expressed higher levels of the checkpoint receptors PD-1, Tim-3 or LAG3 (**Fig. 6B** and **S8**), whose individual expression has been shown to peak at maximal effector phase and reflect CTL activation rather than exhaustion (27,28). Tumor-infiltrating Tetramer$^+$ CD4$^+$ T cells or CTLs harbored decreased percentages of PD-1$^+$ or Tim-3$^+$ cells in mutant mice as compared to control animals, suggesting an incomplete effector differentiation (**Fig. 6B** and **Fig. S8**). This was also the case for Tetramer$^+$ CTLs in TdLN (**Fig. S9**). The co-expression on the same cell of multiple checkpoint receptors, such as PD-1, Tim-3 and LAG3, has been proposed to define functionally exhausted or dysfunctional lymphocytes (27). The proportion of triple-positive cells were very low on both total and Tetramer$^+$ T lymphocytes in all mouse strains, suggesting that the vast majority of anti-tumor T cells were not exhausted (**Fig. S10**). Altogether, these results showed that cDC1 and IFNs were essential to promote CTL and CD4$^+$ T cell effector differentiation in the tumor and TdLNs.

We next compared mouse strains for the ability of their tumor- or TdLN-associated T cells to expand and to produce cytokines upon *ex vivo* Ag-specific re-stimulation. Tumor-infiltrating naïve (CD44$^-$) and activated (CD44$^+$) T_{conv} and CTLs proliferated less in mutant mice than in control animals (**Fig. 6B**). Activated (CD44$^+$) CTLs expressed less Granzyme B, IFN-γ and TNF in mutant mice than in control animals, at all-time points examined in the tumor (**Fig. 6B**) and at day 7 in TdLN (**Fig. 6C**). Altogether, these results showed that IFNs and cDC1 in tumor and TdLN contributed to promote the terminal differentiation of anti-tumor CTLs and CD4$^+$ T_{conv} for the acquisition of protective effector functions.

362

363 **Genes associated to cDC1, CTLs, helper T cells, IFN-I and IFN-γ are associated with a**
364 **better prognosis in human breast cancer patients**

365 We wanted to know whether the immune cells and signaling pathways associated to the immune
366 control of the mouse NOP23 breast adenocarcinoma model were of good prognosis in breast
367 cancer patients. We used the TCGA database to analyze the transcriptomes of human tumors to
368 infer the degree of their infiltration by cDC1 and its association with the clinical outcome.
369 XCR1 is the only marker fully specific for cDC1 in both mice and humans (17,29). The patients
370 who harbored a high *XCR1* expression in their tumor had a significantly better overall survival
371 (**Fig. 7A**), strongly suggesting that a higher cDC1 infiltration in breast tumors was associated
372 with a better prognosis. Patients whose tumor harbored a higher expression of *CCR7* and of its
373 ligand *CCL19* also had a significantly better overall survival (**Fig. 7B**), suggesting that
374 activation of the CCR7/CCL19 axis in human breast tumors promotes more efficient immune
375 responses as shown in the NOP23 mouse model. Finally, we used gene ontology (GO) to
376 determine whether the gene lists associated with a good (n=367, **Fig. 7C**) or bad (n=210, **Fig.**
377 **S11**) prognosis in breast cancer patients were enriched for associations with specific biological
378 processes or signaling pathways. The GO terms enriched in the gene list associated to a good
379 prognosis were linked to the activation and helper or cytotoxic functions of T cell responses as
380 well as to IFN-I and IFN-γ signaling pathways (**Fig. 7C**). Conversely, the GO terms associated
381 to the bad prognosis gene list were linked to mitochondria and translation, likely reflecting
382 active metabolism and proliferation of tumor cells (**Fig. S11**). In conclusion, these analyses
383 strongly suggested that cDC1, $CD4^+$ T cells, CTLs, NK cells and IFNs play together a crucial
384 role in the immune control of breast cancer, not only in the NOP23 mouse model but also in
385 human patients.

386

Discussion

Here, we investigated whether and how cDC1 promote the spontaneous control of breast cancer in mice, by combining mutant animals enabling specific targeting of cDC1 *in vivo* with an orthotopic model of engraftment of the syngeneic breast adenocarcinoma cell line NOP23. Specifically, we investigated how tumor growth and the nature of the immune infiltrate in the tumor or its draining lymph node were affected by a specific, constitutive or conditional, depletion of cDC1, or by the genetic inactivation of candidate input or output signals specifically in cDC1.

We showed unequivocally that cDC1 were required for the CTL-dependent control of the NOP23 breast adenocarcinoma, throughout the entire antitumor immune response, but especially very early on at the time when anti-tumor T cells are primed. We then wondered which molecular mechanisms promoted cDC1 infiltration into the tumor, and their later migration to the draining lymph node. CXCL9 has been proposed to promote infiltration of pre-cDC1 in the tumor bed (30). XCR1 expression by cDC1 can contribute to their recruitment by XCL1-producing NK/NK T cells and CTLs in infected tissues (23,31). However, neither XCR1 nor CXCL9 were individually required for this function in the NOP23 model. Hence, different chemokine receptors may redundantly promote cDC1 recruitment into the tumor bed, close to effector lymphocytes, as observed for XCR1 and CCR5 in melanoma or colorectal tumors in mice (16). The lack of tumor control in *Ccr7*$^{-/-}$ mice could reflect at least in part a strict requirement of this chemokine receptor for cDC1 migration from the tumor to the TdLNs, as previously suggested in a model of melanoma (32).

We then investigated the role of candidate output signals delivered by cDC1 for the promotion of the recruitment of cytotoxic lymphocytes to the tumor and for the activation of their anti-

412 tumor functions. In microbial infections, cDC1 production of high levels of CXCL9 promote
413 the recruitment of effector and memory CTLs expressing CXCR3 in secondary lymphoid
414 organs (22). This has been proposed to be also the case in tumors (33-35). cDC1 are also a
415 major source of IL-12 and IL-15 promoting activation, survival and cytotoxic functions of NK
416 cells and CTLs (22,34-40). However, CXCL9 and IL-12 production as well as IL-15 trans-
417 presentation by cDC1 were individually dispensable for the immune control of the NOP23
418 breast adenocarcinoma. These results suggest a level of redundancy higher than expected
419 between different types of output signals delivered by cDC1. Indeed, CXCL9 and CXCL10 can
420 both promote the recruitment of CXCR3-expressing effector or memory CTLs in inflamed
421 tissues. In our experimental settings, IL-12, IL-15, IL-18 and IFN-I/III or other cytokines might
422 exert overlapping effects for promoting the proliferation, IFN-γ production and cytotoxic
423 activity of NK and CTLs, as had been reported during certain microbial infections (41,42).
424
425 Finally, we sought to identify key input signals required for cDC1 to mediate protective
426 antitumor effects. During microbial infections, the induction of protective NK and T cell
427 responses critically depends on the immunogenic maturation of cDC1, which is driven at least
428 in part by their responses to IFN-I (20) or IFN-γ (22,43,44). Here, we showed that overall IFN-
429 I, IFN-γ and STAT1 responses were critical for rejection of the NOP23 breast adenocarcinoma.
430 Only IFN-γ and STAT1 responses were required to occur in cDC1, whereas cell-intrinsic
431 response to IFN-I in cDC1 were dispensable for tumor rejection. Hence, we show here that
432 IFN-I is not always critical for enhancing cDC1 cross-presentation and more generally for
433 licensing them to promote tumor control. This raises the question of the extent to which cDC1-
434 intrisic IFN-I signaling is critical for effective immunity against cancer, besides for immune-
435 mediated rejection of syngeneic and immunogenic fibrosarcoma and melanoma in mice (18,19).
436 However, cDC1-specific inactivation of *Stat1* led to a higher tumor growth than the loss of IFN-

γ signaling alone, suggesting some level of redundancy between these two activation pathways for the promotion of cDC1 immunogenic maturation. STAT1 is also key in transducing the signal of IFN-III, whose expression is associated with a better prognosis for breast cancer patients, together with the level of cDC1 infiltration in the tumor (45). Moreover, cDC1 are a main source of IFN-III in human breast tumors (45). Hence, it would be interesting in future studies to investigate whether cDC1 produce, and respond to, IFN-III in the NOP23 breast adenocarcinoma model, and how this may contribute to the spontaneous rejection of the tumor. It will also be interesting to investigate whether further boosting cDC1 development and IFN-III production could help improve immune responses against triple negative breast cancer, similarly to what was recently reported in a therapeutic vaccination trial in human melanoma patients (46). Since overall IFN-I responses but not cDC1 responses to IFN-I were essential for the immune control of the NOP23 breast adenocarcinoma, IFN-I must exert critical effect on other immune cells, likely CTL themselves as was reported in microbial infections (42,47,48).

Finally, to attempt better understanding how IFN and cDC1 were promoting immune rejection of the NOP23 breast adenocarcinoma, we examined how their loss affected the immune landscape of the tumor bed and of the TdLN. We observed that cDC1 and IFNs shaped the tumor immune landscape by promoting $CD4^+$ T_{conv} and CTL infiltration and their terminal differentiation with enhanced effector functions. Conversely, cDC1 and IFN responses limited the numbers of putatively deleterious myeloid cell types in the tumor and in TdLN, including, macrophages and neutrophils. In the tumors from *Ifnar1*$^{-/-}$ and *Ifngr1*$^{-/-}$ mice, cDC1 expressed less CD40. Together with our observation of the simultaneous interactions of cDC1 with $CD4^+$ T cells and CTLs in the tumor bed, this suggested that cell-intrinsic responses of cDC1 to IFN may be critical to promote their ability to deliver to CTL the help from $CD4^+$ T_{conv} in a manner depending on their interactions via CD40/CD40L. This hypothesis is consistent with the

462 demonstration that simultaneous presentation of viral antigens by cDC1s to CTLs and $CD4^+$ T
463 cells is key for robust antiviral cellular immunity (49,50) and with publications linking CD40
464 expression on cDC1, their ability to activate $CD4^+$ T_{conv} and the CTL-dependent rejection of
465 tumors (14,51).
466
467 To the best of our knowledge, we show here for the first time in tumors that cDC1 act as a
468 unique cellular platform docking simultaneously $CD4^+$ T_{conv} and CTLs, which is likely key to
469 their ability to relay $CD4^+$ T cell help to CTLs in situ in tumor, akin to what had been previously
470 shown in infectious settings (49,50). We also rigorously demonstrate for the first time that cell-
471 intrinsic signaling by IFN-γ and STAT1 in cDC1 is critical to their anti-tumor functions.
472 Although this had been suggested before (19,52), it was never formally proven due to lack of
473 adequate models to specifically inactivate IFN-γ signaling in cDC1 without also affecting it in
474 other $CD11c^+$ cells. Moreover, in our experimental settings, the licensing of cDC1 by IFN-γ for
475 promoting the control of the NOP23 breast cancer model does not require IL-12 contrary to
476 what has been previously observed or proposed (36,40,52). Beside tumor Ag cross-
477 presentation, the precise nature of the output signals delivered by cDC1 that are critical to
478 induce and maintain protective functions of antitumor $CD4^+$ T_{conv} and CTLs remain to be
479 identified, but may encompass IFN-I/III production and CD40 expression. Future studies based
480 on comparative gene expression profiling of WT versus *Ifngr1*$^{-/-}$ or *Stat1*$^{-/-}$ cDC1 infiltrating
481 the tumor or having migrating to the TdLN should help to identify the output signals whose
482 delivery from cDC1 to effector anti-tumor lymphocytes is critical for the spontaneous rejection
483 of the NOP23 cancer adenocarcinoma model.
484
485 Consistent with our experimental results in mice, human breast cancer patients harboring a high
486 expression in their tumor of genes specific to cDC1, CTL, helper T cells or IFN responses have

a significantly better clinical outcome. Therefore, we propose the following model of how cDC1 promote tumor immunosurveillance (**Fig. S12**). Following tumor cell immunogenic death, cDC1 capture tumor Ag, undergo immunogenic maturation and migrate to the TdLNs in a CCR7-dependent manner to prime $CD4^+$ T_{conv} towards T_H1 and $CD8^+$ T cells towards multipotent protective CTLs. In turn, activated anti-tumor T cells infiltrate the tumor, contributing i) to enhance local recruitment of cDC1, by producing redundant chemokines such as XCL1 and CCL5, and ii) to induce their immunogenic maturation via IFN-γ. This leads to quadripartite interactions in the tumor between cDC1, tumor cells, $CD4^+$ T_{conv} and CTLs, ensuring local amplification and maintenance of the effector functions of anti-tumor T cell responses, leading to tumor eradication. IFN-I and IFN-III produced by the cDC1 themselves or other cells might also redundantly contribute to induce cDC1 immunogenic maturation, together with IFN-γ.

Authors' Contributions

R. Mattiuz: Conceptualization, methodology, investigation, formal analysis, visualization, writing–original draft, writing– review and editing. **C. Brousse:** Resources, investigation. **M. Ambrosini:** Resources, investigation, visualization. **J.-C. Cancel:** Investigation. **Julie Mussard:** investigation. **Amélien Sanlaville:** Resources. **G. Bessou:** Resources, investigation. **C. Caux:** Resources, funding acquisition, methodology, writing– review and editing. **N. Bendriss-Vermare:** Resources, methodology, writing– review and editing. **J. Valladeau-Guilemond:** Resources, methodology, writing– review and editing. **M. Dalod:** Conceptualization, funding acquisition, methodology, supervision, formal analysis, visualization, data curation, validation, writing– review and editing. **K. Crozat:** Conceptualization, funding acquisition, methodology, supervision, investigation, formal analysis, visualization, data curation, validation, writing– review and editing.

Acknowledgments

This work was supported by grants from the ANR (XCR1-DirectingCells to KC), the Fondation pour la Recherche Médicale (label Equipe FRM 2011, project number DEQ20110421284 to MD), the Fondation ARC (to KC), the Institut National du Cancer (INCa PLBIO 2018-152 to CC and MD), and from the European Research Council under the European Community's Seventh Framework Program (FP7/2007–2013 grant agreement number 281225 to MD). This work also benefited from institutional funding by CNRS and INSERM. RM was supported by doctoral fellowships from the Biotrail Ph.D. program (Fondation A*MIDEX) and from Fondation ARC. JCC had a doctoral fellowship from LNCC. We thank Dr. Brad Nelson (Director, Deeley Research Centre, BC Cancer Agency, Victoria BC, Canada) for authorization to use the NOP23 cell line. We thank members of the CIML cytometry, Immagimm and histology facilities and from the CIML/CIPHE mouse houses. We acknowledge France Bio

526 lmaging infrastructure supported by the Agence Nationale de la Recherche (ANR-10-INBS-04-
527 01, call “Investissement d’Avenir”). We thank Hugues Lelouard (CIML) for sharing mice, and
528 Rebecca Gentek and Pierre Golstein (CIML) for helpful discussions and protocols. This work
529 benefited from data assembled by the TCGA, The Human Protein Atlas, and Kaplan Meier-
530 plotter databases. Figure S12 has been created with BioRender (https://biorender.com/) under
531 academic license.

Figures and Figure legends:

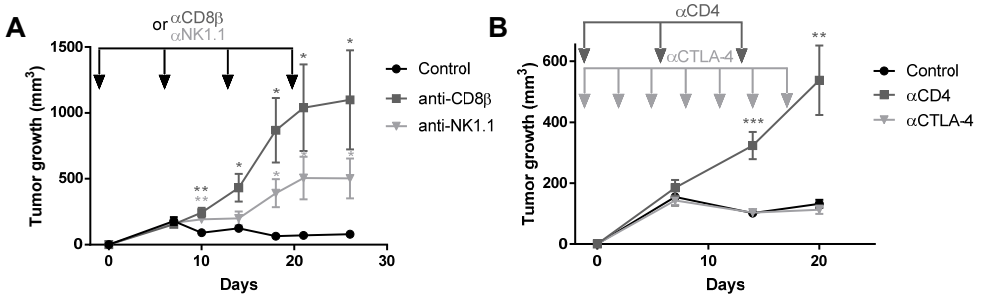

Figure 1.

CTL, CD4$^+$ T_{conv} and NK1.1$^+$ cells are instrumental in spontaneous rejection of breast cancer NOP23. **A**, NOP23 tumor growth in the mammary fat pad of female mice treated or not with anti-CD8β or anti-NK1.1 mAb at the indicated time (arrows) with the first injection given 1d before tumor engraftment. One experiment representative of at least 2 independent ones with 5 mice per group is shown. **B,** NOP23 tumor growth in female mice treated or not with anti-CD4 (once a week) or anti-CTLA-4 (every 3 days) mAb at the indicated time (arrows) with the first injection given 1d before tumor engraftment. n=7 mice per group. *, $p < 0.05$; **, $p < 0.01$; ***, $p < 0.001$ (unpaired *t* test).

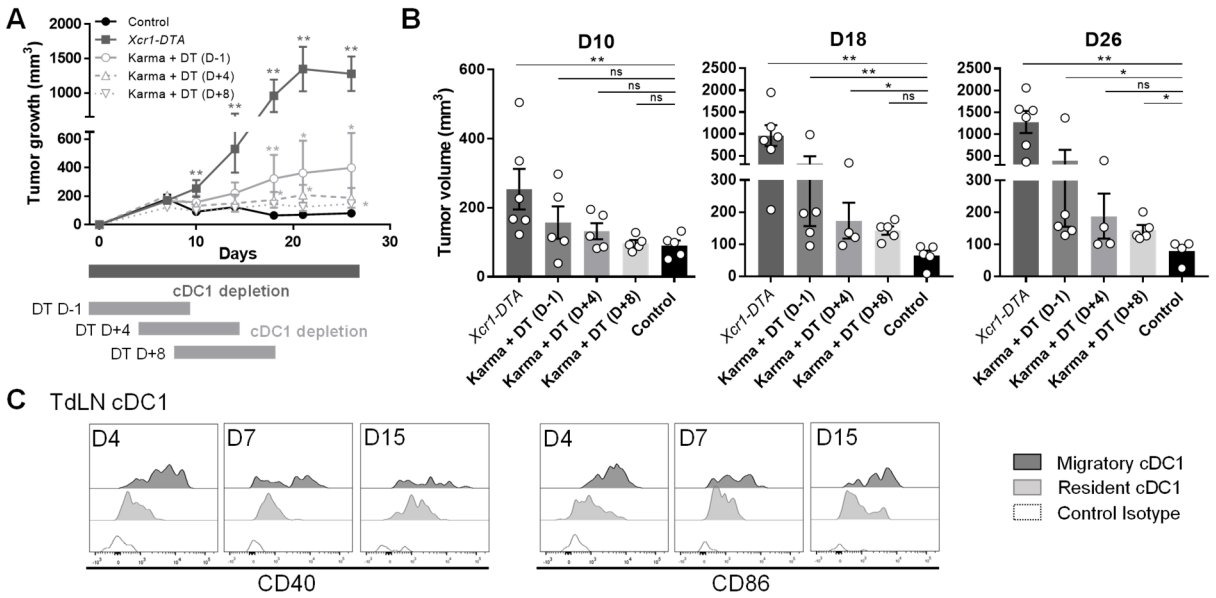

Figure 2.

545 cDC1 are instrumental in spontaneous rejection of breast cancer NOP23, especially during the
546 phase of T cell priming. **A,** Tumor growth in control (n=5), in constitutively cDC1-depleted (*Xcr1-*
547 *DTA*, n=6) or conditionally cDC1-depleted (*Karma-tmt-DTR* + DT) female mice. *Karma-tmt-DTR* mice
548 were injected 4 times with DT every 60h, starting 1d before engraftment (n=5, representative of 3
549 independent datasets), at d+4 post-engraftment (n=5, representative of 2 independent datasets), or at d+8
550 post engraftment (n=5, representative of 2 independent datasets). **B,** Tumor volumes as measured in
551 panel (A) at day 10, 18 and 26. ns, not significant ($p > 0.05$); *, $p < 0.05$; **, $p < 0.01$; ***, $p < 0.001$;
552 (non-parametric Mann–Whitney test). **C,** Analysis of CD40 and CD86 expression by flow cytometry on
553 TdLN Mig-cDC1 and Res-cDC1. The data shown are from one experiment representative of two
554 independent ones.
555

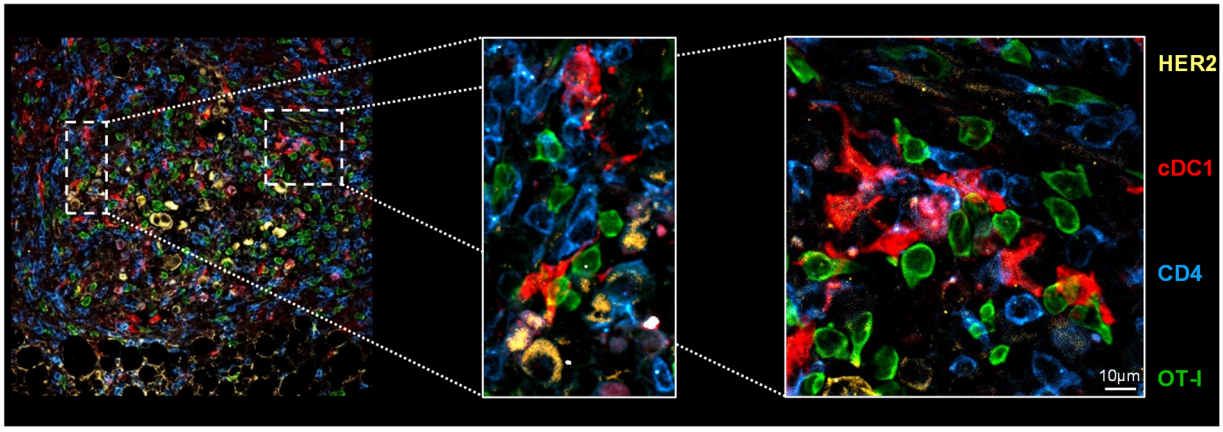

556 cDC1 RFP+ (*Xcr1*$^{Cre/wt}$; *Rosa26*$^{tdRFP/wt}$) / OT-I GFP+ / CD4+ T cells / NOP23 HER2+ at Day 7 post tumor engraftment

557 **Figure 3.**

558 cDC1 interact with CD4$^+$ T and tumor-specific CD8$^+$ T cells together in the tumor
559 microenvironment. *Xcr1*$^{Cre/wt}$;*Rosa26*$^{tdRFP/wt}$ mice were adoptively transferred with 1,000 GFP$^+$ OT-I
560 cells 1d prior to tumor engraftment. 7d post-engraftment, tumors sections were stained for RFP
561 expression (cDC1), GFP (OT-I), CD4 (CD4$^+$ T cells) and HER2 (NOP23 cells). This image is
562 representative of 5 individual mice.
563
564

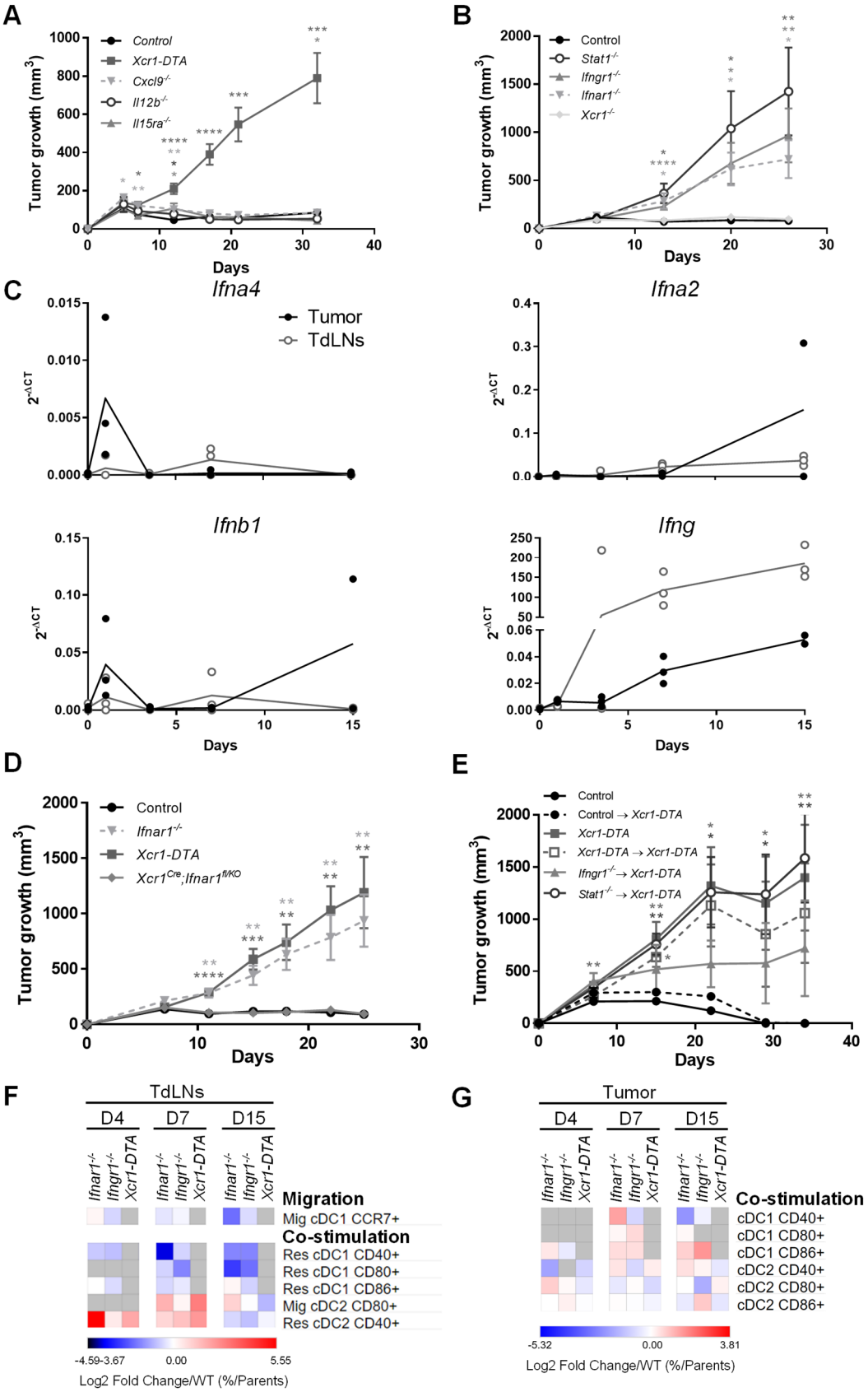

Figure 4.

IFNs and cDC1-intrinsic IFN-γ and STAT1 signaling are necessary for breast cancer spontaneous rejection. **A,** Tumor growth in *Xcr1-DTA* (n=10), *Cxcl9*$^{-/-}$ (n=9), *Il12b*$^{-/-}$ (n=6), *Il15ra*$^{-/-}$ (n=5) and control (n=8) female mice. One experiment representative of two independent ones is shown. **B,** Tumor growth in *Xcr1*$^{-/-}$ (n=4), *Ifnar1*$^{-/-}$ (n=7), *Ifngr1*$^{-/-}$ (n=5), *Stat1*$^{-/-}$ (n=5) and control (n=6) female mice. One experiment representative of at least 2 independent ones is shown. **C,** Expression analysis of the *Ifna4*, *Ifna2*, *Ifnb* and *Ifng* genes in control tumors and their TdLNs (n=2-4) by qPCR. **D,** Tumor growth in *Xcr1-DTA* (n=7), *Ifnar1*$^{-/-}$ (n=8), *Xcr1*^{cre};*Ifnar1*$^{fl/KO}$ (n=13) and control (n=7) female mice. One experiment representative of two independent ones is shown. **E,** Tumor growth in different types of shield bone marrow chimera female mice, control→*Xcr1-DTA* (n=4), *Xcr1-DTA*→*Xcr1-DTA* (n=4), *Ifngr1*$^{-/-}$→*Xcr1-DTA* (n=4) and *Stat1*$^{-/-}$→*Xcr1-DTA* (n=4). *Xcr1-DTA* (n=5) and control (n=5) female mice were used as controls. One experiment representative of two independent ones is shown. *, $P < 0.05$; **, $P < 0.01$; ***, $P < 0.001$; ****, $P < 0.0001$ (unpaired *t* test). **F-G,** Heatmaps representing the expression of co-stimulatory receptors on lymphoid resident (res) and migratory (Mig) cDC1 and cDC2 in the TdLNs (**F**) and tumors (**G**) at d4, d7 and d15 after engraftment in *Ifnar1*$^{-/-}$, *Ifngr1*$^{-/-}$, *Xcr1-DTA* compared to control mice. The data are shown as Log2 Fold Changes in the ratio of % Population/Parent population from mutant animals to WT (n=3-6 mice per group). The data shown are from two independent experiments pooled together.

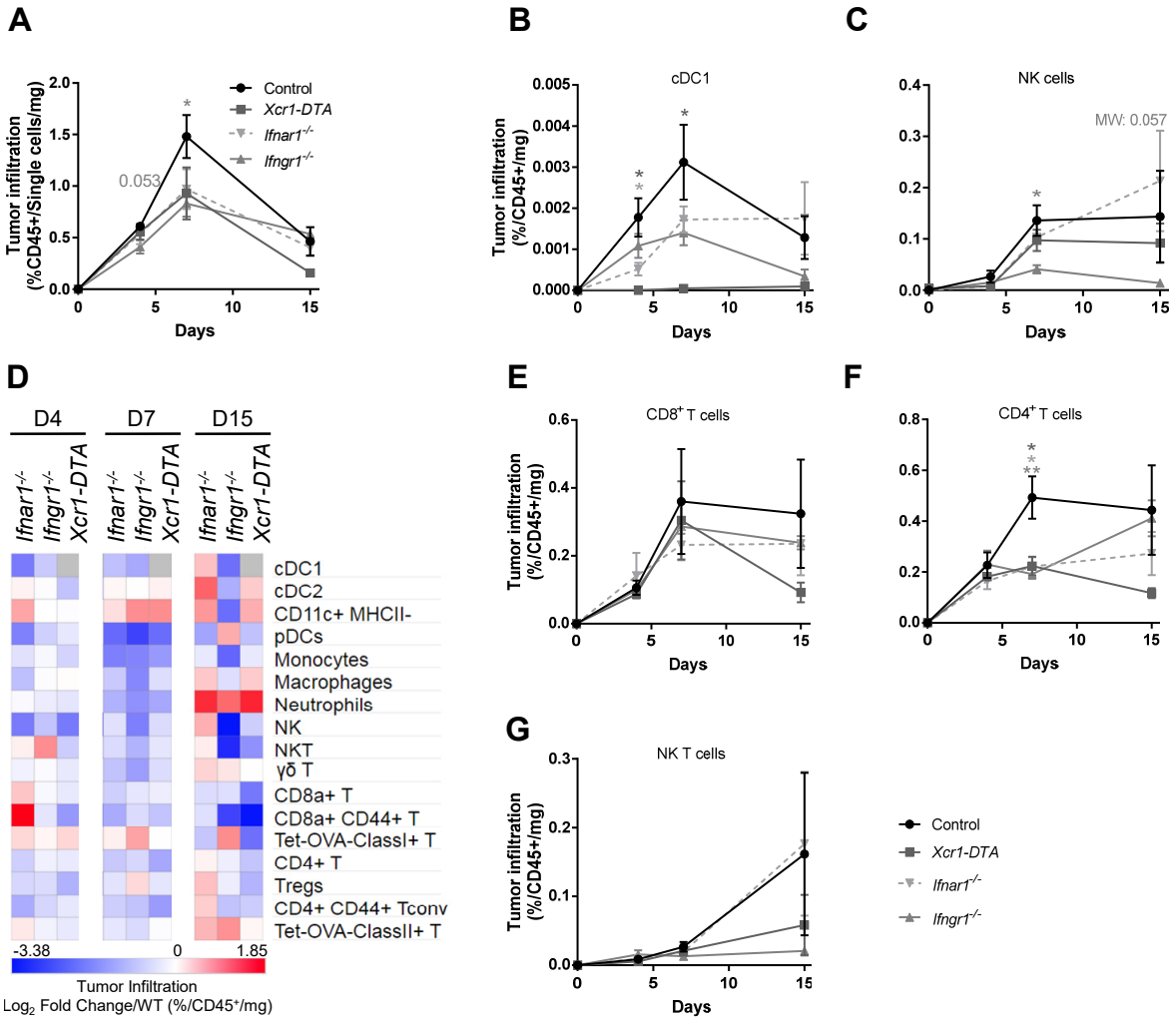

Figure 5.

cDC1, type I IFN and type II IFN signaling shape the tumor immune landscape. **A,** Kinetics of the tumor infiltration by CD45$^+$ cells at d4, d7 and d15, in control, *Ifnar1*$^{-/-}$, *Ifngr1*$^{-/-}$ and *Xcr1-DTA* mice, as assessed by flow cytometry. **B-C,** Kinetics of the tumor infiltration by cDC1 (B) and NK cells (D) at d4, d7 and d15, in control, *Ifnar1*$^{-/-}$, *Ifngr1*$^{-/-}$ and *Xcr1-DTA* mice. **D,** Heatmap representing the tumor immune landscapes in *Ifnar1*$^{-/-}$, *Ifngr1*$^{-/-}$ and *Xcr1-DTA* mice at d4, d7 and d15. The data are shown as Log2 Fold Changes calculated as the ratio of % Population/CD45$^+$/mg of tumor from mutant animals to WT (n=3-6 mice per group). The data shown are from two independent experiments pooled together. **E-G,** Kinetics of the tumor infiltration by CD8$^+$ T cells (**E**), CD4$^+$ T cells (**F**) and NK T cells (**G**) in control, *Ifnar1*$^{-/-}$, *Ifngr1*$^{-/-}$ and *Xcr1-DTA* mice. For (A-C) and (E-G), the data shown (mean+/-SEM) are from two independent experiments pooled together (n=3-6 mice per group). ns, not significant (p >

0.05); *, p < 0.05; **, p < 0.01; ***, p < 0.001 according to unpaired *t* test or nonparametric Mann–Whitney test (MW) when specified.

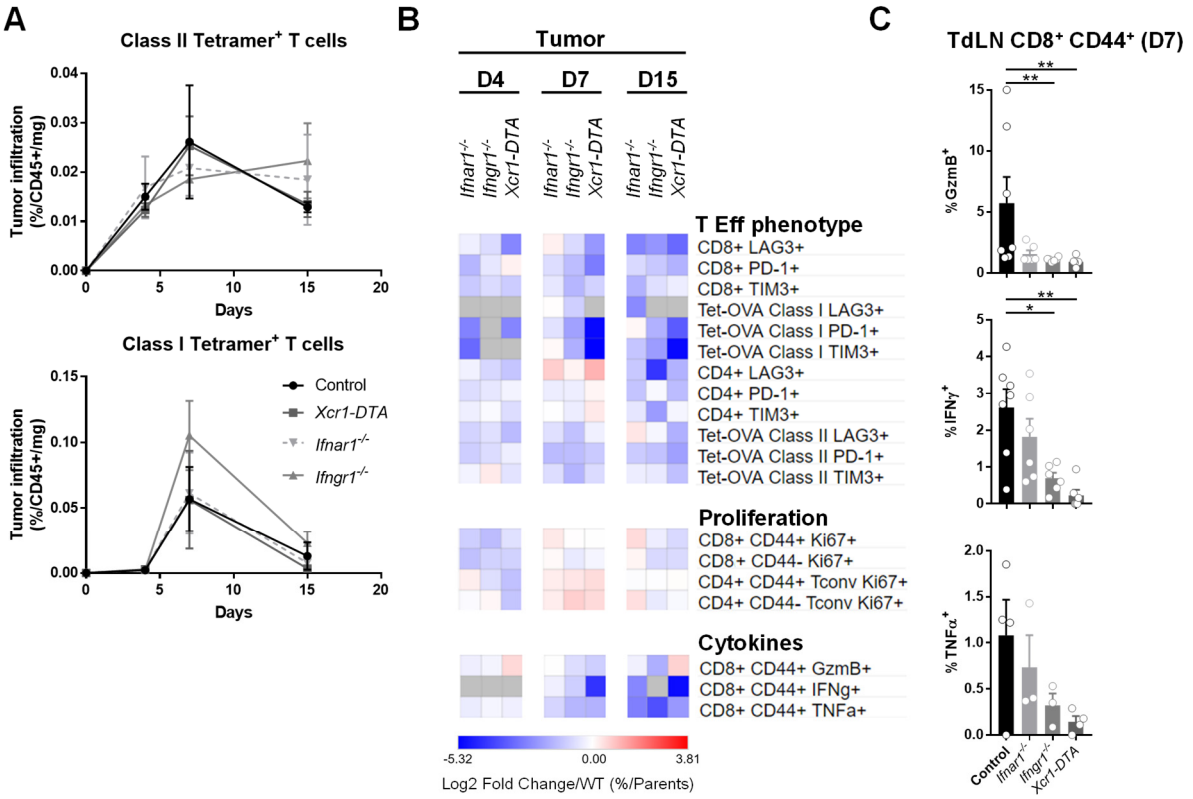

Figure 6.

cDC1, type I IFN and type II IFN signaling are necessary for $CD4^+$ and $CD8^+$ T cell terminal activation and effector functions in the TME. **A,** Kinetics of the tumor infiltration by Ag-specific $CD4^+$ (up) and $CD8^+$ (bottom) T cells at d4, d7 and d15 in *Ifnar1*$^{-/-}$, *Ifngr1*$^{-/-}$ *Xcr1-DTA* and control mice. The data shown (mean+/-SEM) are from two independent experiments pooled together (n=3-6 mice per group). **B,** Heatmap representing T cell effector phenotype and proliferation, and CTL cytokine production. The data are shown as Log2 Fold Changes in the ratio of % Population/Parent population from mutant animals to WT (n=3-6 mice per group). **C,** Expression of GzmB, IFN-γ and TNFα by OVA-specific $CD44^+$ $CD8^+$ T cells in the TdLN of *Ifnar1*$^{-/-}$, *Ifngr1*$^{-/-}$ *Xcr1-DTA* and control mice day 7 post-engraftment. The data shown are from two independent experiments pooled together. *, p < 0.05; **, p < 0.01; ***, p < 0.001; (non-parametric Mann–Whitney test).

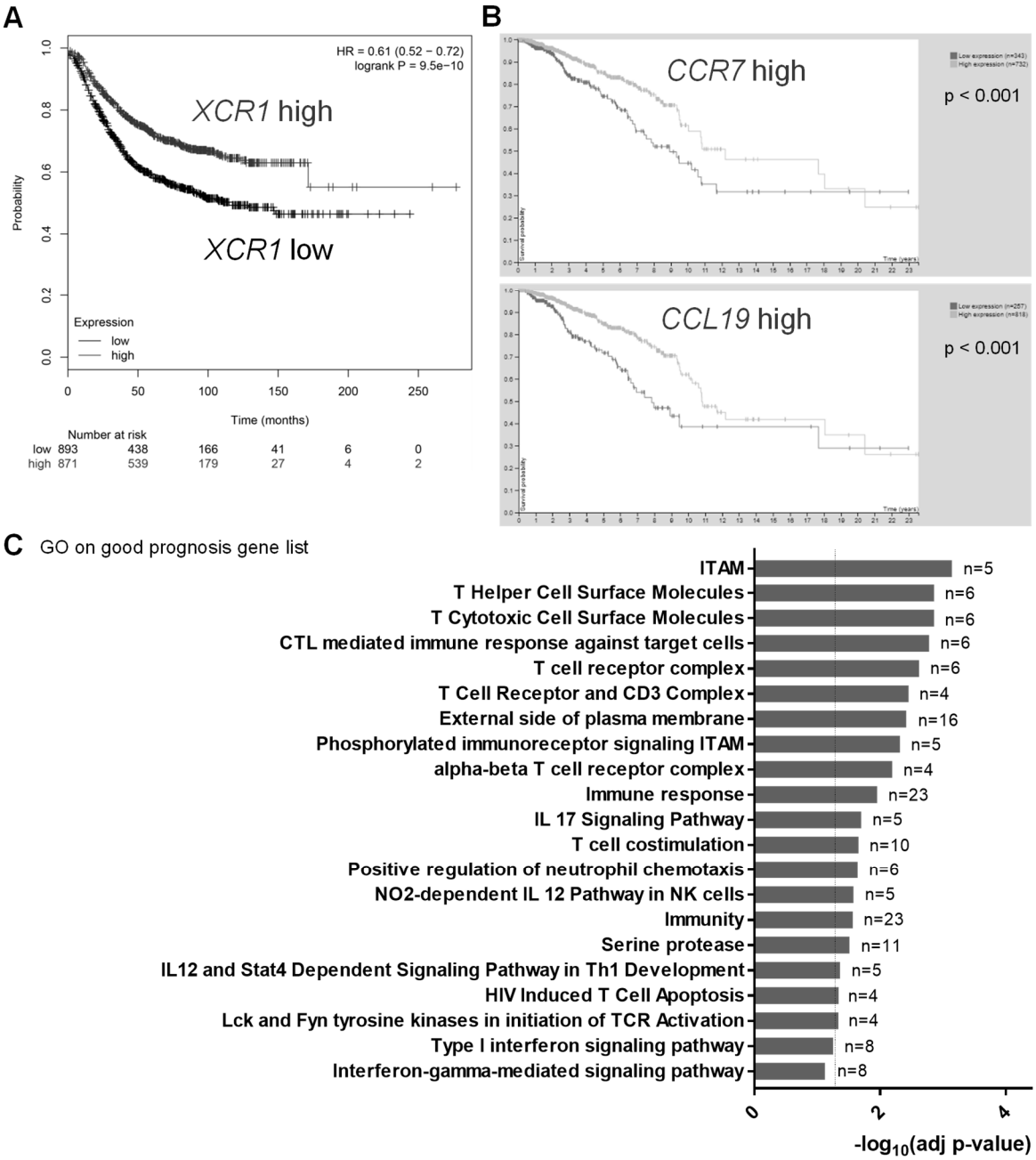

Figure 7.

Intratumor expression of *XCR1* and gene ontology annotations linked to CTL, Helper T cell and IFN-I/II signaling are all associated to a better prognosis in human breast cancer patients. **A-B,** Kaplan Meier plot of *XCR1* expression (**A**), and of *CCR7* and *CCL19* expression (**B**) in human breast cancer. **C,** Gene Ontology of breast cancer good prognosis gene set performed with DAVID 6.8. A gene is considered prognostic if correlation analysis of gene expression and clinical outcome resulted in Kaplan-Meier plots with high significance ($p<0.001$). (A) is from Kaplan Meier-plotter database, (B) and (C) data from the TCGA database.

References

1. Vu Manh TP, Bertho N, Hosmalin A, Schwartz-Cornil I, Dalod M. Investigating Evolutionary Conservation of Dendritic Cell Subset Identity and Functions. Front Immunol **2015**;6:260 doi 10.3389/fimmu.2015.00260.
2. Sancho D, Joffre OP, Keller AM, Rogers NC, Martinez D, Hernanz-Falcon P*, et al.* Identification of a dendritic cell receptor that couples sensing of necrosis to immunity. Nature **2009**;458(7240):899-903 doi 10.1038/nature07750.
3. Theisen DJ, Davidson JTt, Briseno CG, Gargaro M, Lauron EJ, Wang Q*, et al.* WDFY4 is required for cross-presentation in response to viral and tumor antigens. Science **2018**;362(6415):694-9 doi 10.1126/science.aat5030.
4. Laoui D, Keirsse J, Morias Y, Van Overmeire E, Geeraerts X, Elkrim Y*, et al.* The tumour microenvironment harbours ontogenically distinct dendritic cell populations with opposing effects on tumour immunity. Nat Commun **2016**;7:13720 doi 10.1038/ncomms13720.
5. Cancel JC, Crozat K, Dalod M, Mattiuz R. Are Conventional Type 1 Dendritic Cells Critical for Protective Antitumor Immunity and How? Front Immunol **2019**;10:9 doi 10.3389/fimmu.2019.00009.
6. Wculek SK, Cueto FJ, Mujal AM, Melero I, Krummel MF, Sancho D. Dendritic cells in cancer immunology and immunotherapy. Nat Rev Immunol **2020**;20(1):7-24 doi 10.1038/s41577-019-0210-z.
7. Sichien D, Scott CL, Martens L, Vanderkerken M, Van Gassen S, Plantinga M*, et al.* IRF8 Transcription Factor Controls Survival and Function of Terminally Differentiated Conventional and Plasmacytoid Dendritic Cells, Respectively. Immunity **2016**;45(3):626-40 doi 10.1016/j.immuni.2016.08.013.
8. Bosteels C, Neyt K, Vanheerswynghels M, van Helden MJ, Sichien D, Debeuf N*, et al.* Inflammatory Type 2 cDCs Acquire Features of cDC1s and Macrophages to Orchestrate Immunity to Respiratory Virus Infection. Immunity **2020**;52(6):1039-56 e9 doi 10.1016/j.immuni.2020.04.005.
9. Hildner K, Edelson BT, Purtha WE, Diamond M, Matsushita H, Kohyama M*, et al.* Batf3 deficiency reveals a critical role for CD8alpha+ dendritic cells in cytotoxic T cell immunity. Science **2008**;322(5904):1097-100 doi 10.1126/science.1164206.
10. Lee W, Kim HS, Hwang SS, Lee GR. The transcription factor Batf3 inhibits the differentiation of regulatory T cells in the periphery. Exp Mol Med **2017**;49(11):e393 doi 10.1038/emm.2017.157.
11. Ataide MA, Komander K, Knopper K, Peters AE, Wu H, Eickhoff S*, et al.* BATF3 programs CD8(+) T cell memory. Nat Immunol **2020**;21(11):1397-407 doi 10.1038/s41590-020-0786-2.
12. Qiu Z, Khairallah C, Romanov G, Sheridan BS. Cutting Edge: Batf3 Expression by CD8 T Cells Critically Regulates the Development of Memory Populations. J Immunol **2020**;205(4):901-6 doi 10.4049/jimmunol.2000228.
13. Mattiuz R, Wohn C, Ghilas S, Ambrosini M, Alexandre YO, Sanchez C*, et al.* Novel Cre-Expressing Mouse Strains Permitting to Selectively Track and Edit Type 1 Conventional Dendritic Cells Facilitate Disentangling Their Complexity in vivo. Front Immunol **2018**;9:2805 doi 10.3389/fimmu.2018.02805.
14. Ferris ST, Durai V, Wu R, Theisen DJ, Ward JP, Bern MD*, et al.* cDC1 prime and are licensed by CD4(+) T cells to induce anti-tumour immunity. Nature **2020**;584(7822):624-9 doi 10.1038/s41586-020-2611-3.
15. Balan S, Radford KJ, Bhardwaj N. Unexplored horizons of cDC1 in immunity and tolerance. Adv Immunol **2020**;148:49-91 doi 10.1016/bs.ai.2020.10.002.

16. Bottcher JP, Bonavita E, Chakravarty P, Blees H, Cabeza-Cabrerizo M, Sammicheli S, *et al.* NK Cells Stimulate Recruitment of cDC1 into the Tumor Microenvironment Promoting Cancer Immune Control. Cell **2018**;172(5):1022-37 e14 doi 10.1016/j.cell.2018.01.004.
17. Crozat K, Guiton R, Contreras V, Feuillet V, Dutertre CA, Ventre E, *et al.* The XC chemokine receptor 1 is a conserved selective marker of mammalian cells homologous to mouse CD8alpha+ dendritic cells. J Exp Med **2010**;207(6):1283-92 doi 10.1084/jem.20100223.
18. Diamond MS, Kinder M, Matsushita H, Mashayekhi M, Dunn GP, Archambault JM, *et al.* Type I interferon is selectively required by dendritic cells for immune rejection of tumors. J Exp Med **2011**;208(10):1989-2003 doi 10.1084/jem.20101158.
19. Fuertes MB, Kacha AK, Kline J, Woo SR, Kranz DM, Murphy KM, *et al.* Host type I IFN signals are required for antitumor CD8+ T cell responses through CD8{alpha}+ dendritic cells. J Exp Med **2011**;208(10):2005-16 doi 10.1084/jem.20101159.
20. Tomasello E, Pollet E, Vu Manh TP, Uze G, Dalod M. Harnessing Mechanistic Knowledge on Beneficial Versus Deleterious IFN-I Effects to Design Innovative Immunotherapies Targeting Cytokine Activity to Specific Cell Types. Front Immunol **2014**;5:526 doi 10.3389/fimmu.2014.00526.
21. Martin ML, Wall EM, Sandwith E, Girardin A, Milne K, Watson PH, *et al.* Density of tumour stroma is correlated to outcome after adoptive transfer of CD4+ and CD8+ T cells in a murine mammary carcinoma model. Breast Cancer Res Treat **2010**;121(3):753-63 doi 10.1007/s10549-009-0559-y.
22. Alexandre YO, Ghilas S, Sanchez C, Le Bon A, Crozat K, Dalod M. XCR1+ dendritic cells promote memory CD8+ T cell recall upon secondary infections with Listeria monocytogenes or certain viruses. J Exp Med **2016**;213(1):75-92 doi 10.1084/jem.20142350.
23. Ghilas S, Ambrosini M, Cancel J-C, Massé M, Lelouard H, Dalod M, *et al.* NK cells orchestrate splenic cDC1 migration to potentiate antiviral protective CD8+ T cell responses. bioRxiv **2020**:2020.04.23.057463 doi 10.1101/2020.04.23.057463.
24. Simpson TR, Li F, Montalvo-Ortiz W, Sepulveda MA, Bergerhoff K, Arce F, *et al.* Fc-dependent depletion of tumor-infiltrating regulatory T cells co-defines the efficacy of anti-CTLA-4 therapy against melanoma. J Exp Med **2013**;210(9):1695-710 doi 10.1084/jem.20130579.
25. Matloubian M, Lo CG, Cinamon G, Lesneski MJ, Xu Y, Brinkmann V, *et al.* Lymphocyte egress from thymus and peripheral lymphoid organs is dependent on S1P receptor 1. Nature **2004**;427(6972):355-60 doi 10.1038/nature02284.
26. Schlitzer A, Sivakamasundari V, Chen J, Sumatoh HR, Schreuder J, Lum J, *et al.* Identification of cDC1- and cDC2-committed DC progenitors reveals early lineage priming at the common DC progenitor stage in the bone marrow. Nat Immunol **2015**;16(7):718-28 doi 10.1038/ni.3200.
27. Blank CU, Haining WN, Held W, Hogan PG, Kallies A, Lugli E, *et al.* Defining 'T cell exhaustion'. Nat Rev Immunol **2019**;19(11):665-74 doi 10.1038/s41577-019-0221-9.
28. Singer M, Wang C, Cong L, Marjanovic ND, Kowalczyk MS, Zhang H, *et al.* A Distinct Gene Module for Dysfunction Uncoupled from Activation in Tumor-Infiltrating T Cells. Cell **2016**;166(6):1500-11 e9 doi 10.1016/j.cell.2016.08.052.
29. Bachem A, Guttler S, Hartung E, Ebstein F, Schaefer M, Tannert A, *et al.* Superior antigen cross-presentation and XCR1 expression define human CD11c+CD141+ cells as homologues of mouse CD8+ dendritic cells. J Exp Med **2010**;207(6):1273-81 doi 10.1084/jem.20100348.

30. Cook SJ, Lee Q, Wong AC, Spann BC, Vincent JN, Wong JJ, *et al.* Differential chemokine receptor expression and usage by pre-cDC1 and pre-cDC2. Immunol Cell Biol **2018**;96(10):1131-9 doi 10.1111/imcb.12186.
31. Brewitz A, Eickhoff S, Dahling S, Quast T, Bedoui S, Kroczek RA, *et al.* CD8(+) T Cells Orchestrate pDC-XCR1(+) Dendritic Cell Spatial and Functional Cooperativity to Optimize Priming. Immunity **2017**;46(2):205-19 doi 10.1016/j.immuni.2017.01.003.
32. Roberts EW, Broz ML, Binnewies M, Headley MB, Nelson AE, Wolf DM, *et al.* Critical Role for CD103(+)/CD141(+) Dendritic Cells Bearing CCR7 for Tumor Antigen Trafficking and Priming of T Cell Immunity in Melanoma. Cancer Cell **2016**;30(2):324-36 doi 10.1016/j.ccell.2016.06.003.
33. Spranger S, Dai D, Horton B, Gajewski TF. Tumor-Residing Batf3 Dendritic Cells Are Required for Effector T Cell Trafficking and Adoptive T Cell Therapy. Cancer Cell **2017**;31(5):711-23 e4 doi 10.1016/j.ccell.2017.04.003.
34. de Mingo Pulido A, Gardner A, Hiebler S, Soliman H, Rugo HS, Krummel MF, *et al.* TIM-3 Regulates CD103(+) Dendritic Cell Function and Response to Chemotherapy in Breast Cancer. Cancer Cell **2018**;33(1):60-74 e6 doi 10.1016/j.ccell.2017.11.019.
35. Bergamaschi C, Pandit H, Nagy BA, Stellas D, Jensen SM, Bear J, *et al.* Heterodimeric IL-15 delays tumor growth and promotes intratumoral CTL and dendritic cell accumulation by a cytokine network involving XCL1, IFN-gamma, CXCL9 and CXCL10. J Immunother Cancer **2020**;8(1) doi 10.1136/jitc-2020-000599.
36. Broz ML, Binnewies M, Boldajipour B, Nelson AE, Pollack JL, Erle DJ, *et al.* Dissecting the tumor myeloid compartment reveals rare activating antigen-presenting cells critical for T cell immunity. Cancer Cell **2014**;26(5):638-52 doi 10.1016/j.ccell.2014.09.007.
37. Beavis PA, Henderson MA, Giuffrida L, Davenport AJ, Petley EV, House IG, *et al.* Dual PD-1 and CTLA-4 Checkpoint Blockade Promotes Antitumor Immune Responses through CD4(+)Foxp3(-) Cell-Mediated Modulation of CD103(+) Dendritic Cells. Cancer Immunol Res **2018**;6(9):1069-81 doi 10.1158/2326-6066.CIR-18-0291.
38. Greyer M, Whitney PG, Stock AT, Davey GM, Tebartz C, Bachem A, *et al.* T Cell Help Amplifies Innate Signals in CD8(+) DCs for Optimal CD8(+) T Cell Priming. Cell Rep **2016**;14(3):586-97 doi 10.1016/j.celrep.2015.12.058.
39. Mittal D, Vijayan D, Putz EM, Aguilera AR, Markey KA, Straube J, *et al.* Interleukin-12 from CD103(+) Batf3-Dependent Dendritic Cells Required for NK-Cell Suppression of Metastasis. Cancer Immunol Res **2017**;5(12):1098-108 doi 10.1158/2326-6066.CIR-17-0341.
40. Ruffell B, Chang-Strachan D, Chan V, Rosenbusch A, Ho CM, Pryer N, *et al.* Macrophage IL-10 blocks CD8+ T cell-dependent responses to chemotherapy by suppressing IL-12 expression in intratumoral dendritic cells. Cancer Cell **2014**;26(5):623-37 doi 10.1016/j.ccell.2014.09.006.
41. Cousens LP, Peterson R, Hsu S, Dorner A, Altman JD, Ahmed R, *et al.* Two roads diverged: interferon alpha/beta- and interleukin 12-mediated pathways in promoting T cell interferon gamma responses during viral infection. J Exp Med **1999**;189(8):1315-28 doi 10.1084/jem.189.8.1315.
42. Thompson LJ, Kolumam GA, Thomas S, Murali-Krishna K. Innate inflammatory signals induced by various pathogens differentially dictate the IFN-I dependence of CD8 T cells for clonal expansion and memory formation. J Immunol **2006**;177(3):1746-54 doi 10.4049/jimmunol.177.3.1746.
43. Lee SH, Carrero JA, Uppaluri R, White JM, Archambault JM, Lai KS, *et al.* Identifying the initiating events of anti-Listeria responses using mice with conditional loss of IFN-

gamma receptor subunit 1 (IFNGR1). J Immunol **2013**;191(8):4223-34 doi 10.4049/jimmunol.1300910.

44. Deauvieau F, Ollion V, Doffin AC, Achard C, Fonteneau JF, Verronese E*, et al.* Human natural killer cells promote cross-presentation of tumor cell-derived antigens by dendritic cells. Int J Cancer **2015**;136(5):1085-94 doi 10.1002/ijc.29087.

45. Hubert M, Gobbini E, Couillault C, Manh TV, Doffin AC, Berthet J*, et al.* IFN-III is selectively produced by cDC1 and predicts good clinical outcome in breast cancer. Sci Immunol **2020**;5(46) doi 10.1126/sciimmunol.aav3942.

46. Bhardwaj N, Friedlander PA, Pavlick AC, Ernstoff MS, Gastman BR, Hanks BA*, et al.* Flt3 ligand augments immune responses to anti-DEC-205-NY-ESO-1 vaccine through expansion of dendritic cell subsets. Nature Cancer **2020**;1(12):1204-17 doi 10.1038/s43018-020-00143-y.

47. Kolumam GA, Thomas S, Thompson LJ, Sprent J, Murali-Krishna K. Type I interferons act directly on CD8 T cells to allow clonal expansion and memory formation in response to viral infection. J Exp Med **2005**;202(5):637-50 doi 10.1084/jem.20050821.

48. Havenar-Daughton C, Kolumam GA, Murali-Krishna K. Cutting Edge: The direct action of type I IFN on CD4 T cells is critical for sustaining clonal expansion in response to a viral but not a bacterial infection. J Immunol **2006**;176(6):3315-9 doi 10.4049/jimmunol.176.6.3315.

49. Eickhoff S, Brewitz A, Gerner MY, Klauschen F, Komander K, Hemmi H*, et al.* Robust Anti-viral Immunity Requires Multiple Distinct T Cell-Dendritic Cell Interactions. Cell **2015**;162(6):1322-37 doi 10.1016/j.cell.2015.08.004.

50. Hor JL, Whitney PG, Zaid A, Brooks AG, Heath WR, Mueller SN. Spatiotemporally Distinct Interactions with Dendritic Cell Subsets Facilitates CD4+ and CD8+ T Cell Activation to Localized Viral Infection. Immunity **2015**;43(3):554-65 doi 10.1016/j.immuni.2015.07.020.

51. Yamauchi T, Hoki T, Oba T, Attwood K, Cao X, Ito F. CD40 and CD80/86 signaling in cDC1s mediate effective neoantigen vaccination and generation of antigen-specific CX3CR1+ CD8+ T cells in mice. bioRxiv **2020**:2020.06.15.151787 doi 10.1101/2020.06.15.151787.

52. Garris CS, Arlauckas SP, Kohler RH, Trefny MP, Garren S, Piot C*, et al.* Successful Anti-PD-1 Cancer Immunotherapy Requires T Cell-Dendritic Cell Crosstalk Involving the Cytokines IFN-gamma and IL-12. Immunity **2018**;49(6):1148-61 e7 doi 10.1016/j.immuni.2018.09.024.